Electronic Supplementary Material (ESI)

A new method for the preparation of $[Sn_2(H_2PO_2)_3]Br$ SHG-active polar crystal by surfactant-induced strategy

Jie-Ling Xie,[#a] Yu-Hua Zhou,[#c] Long-Hua Li,[b*] Jian-Han Zhang[d] and Jun-Ling Song[a*]

[a]School of Chemical & Material Engineering, Jiangnan University, Wuxi 214122, People's Republic of China,

[b]School of Chemistry and Chemical Engineering, Jiangsu University, Zhenjiang 212013, P. R. China,

[c]School of Materials Science and Engineering, Nanyang Technological University, Singapore 639798, Singapore.

[d]School of resources & chemical engineering, Sanming University, Sanming, Fujian, P. R. China, 365004

[#] These authors contributed equally to this work.

*To whom correspondence should be addressed. E-mail: longhuali@ujs.edu.cn, S070054@e.ntu.edu.sg

S1. Experimental Section

All the chemicals used were analytically pure from Shanghai Reagent Factory without further purification.

(1) **Synthesis of $[Sn_2(H_2PO_2)_3]Br$**

Firstly, SnO (4.0 mmol, AR), 4.0 mL H_3PO_2 (50%，about 40.0 mmol H_3PO_2) and 4.0 mL HBr (30%,) were mixed and stirred at 60℃ for 2 hours. Secondly, 10.0 mL octylamine, as a surfactant, was added drop by drop into the mixed solution in 75℃ water bath while witnessed some yellow

plate crystal separate out and dissolved rapidly. After the reaction, the semitransparent solution was cooled down and crystallized under ambient condition in 2~3 days. Finally, transparent and rod-like crystal was obtained and remain stable in ambient atmosphere for six months.

To gain more insight in the influence of long-chain alkyl amine in the synthesis process, we also conducted a blank experiment without octylamine and nothing crystalized from the precursor solution. Besides, the use of other alkyl amine, including butyl amine and dodecyl amine, could not control the crystallization process and fabricate the similar 1D crystal as octlyamine.

S2. Computational Method

Electronic structures calculations are performed by the Vienna Ab initio simulation package (VASP)[1] in the framework of density functional theory (DFT). The general gradient approximation (GGA) functional of Perdew-Burke-Ernzerhof (PBE)[2] is employed. The plane wave basis with the frozen-core projector augmented wave (PAW)[3, 4] potential and a plane wave cut off energy of 400 eV are used. The conjugated gradient method and a 5 × 3 × 2 Monkhorst-Pack *k* mesh are used in the structural optimization. The geometry is fully relaxed until the residual Hellmann-Feynman forces on each atom become smaller than 0.01 eV/Å. After relaxations, we performed the ground state calculation. Then a dense *k* grid of 7 × 6 × 3 is employed in the calculation of density of states (DOS). The second order nonlinear optical susceptibilities are obtained based on the sum-over-states approach[5]. A total 90 *k*-points (12 × 9 × 5) in the irreducible Brillouin zone (IBZ) and 100 unoccupied bands are applied to generate the momentum matrix elements, which are used in the latter nonlinear optical calculation. The contributions to the SHG susceptibility are the interband transitions $\chi_{inter}(2\omega, \omega, \omega)$, the intraband transitions $\chi_{intra}(2\omega, \omega, \omega)$ and the modulation terms $\chi_{mod}(2\omega, \omega, \omega)$. These terms are numbered according to Eqs. (49)–(51) of Ref. 5 and then the SHG

susceptibility tensor is obtained by summing up all these terms.

Supplementary Figures and Tables

Table S1 Crystal data and structural refinement for **1**.

Empirical formula	$[Sn_2(H_2PO_2)_3]Br$
Formula weight	512.28
Temperature	293(2) K
Wavelength	0.71073 Å
Crystal system,	Orthorhombic
Space group	$Pmn2_1$
a/Å	5.4177(4)
b/Å	7.1467(7)
c/Å	13.8359(12)
V/Å^3	535.71(8)
Z	2
D_c/g·cm^{-3}	3.176
μ(Mo Kα)/mm^{-1}	8.829
F(000)	468
Reflections collected / unique	2807 / 1128 [R(int) = 0.0359]
Completeness	99.6 % to theta = 27.42
Data / restraints / parameters	1128 / 1 / 68
Goodness-of-fit on F^2	1.067
Final R indices [I>2sigma(I)][a] R indices (all data)	R_1 = 0.0317, wR_2 = 0.0834 R1 = 0.0326, wR2 = 0.0841
Extinction coefficient	0.021(2)
Absolute structure parameter	0.05(3)

Largest diff. peak and hole	0.813 and -0.978 e. Å^{-3}

[a] $R_1 = \Sigma||F_o|-|F_c||/\Sigma|F_o|$, $\omega R_2 = \{\Sigma\omega[(F_o)^2\ (F_c)^2]^2/\Sigma\omega[(F_o)^2]^2\}^{1/2}$.

Table S2. Atomic coordinates (×10^4) and equivalent isotropic displacement parameters (Å^2×10^3) for **1**. U_{eq} is defined as one third of the trace of the orthogonalized U_{ij} tensor.

Atom	x	y	z	U(eq)
Sn(2)	10000	5231(1)	7236(1)	23(1)
Sn(1)	10000	9572(1)	5542(1)	25(1)
P(1)	5000	5064(4)	8692(2)	22(1)
P(2)	10000	9851(4)	7942(3)	66(2)
P(3)	15000	12575(4)	5489(2)	29(1)
O(1)	7357(10)	4260(9)	8275(4)	34(1)
O(3)	10000	10752(11)	6965(5)	30(2)
O(4)	12635(10)	11693(9)	5165(4)	36(1)
O(2)	10000	7793(10)	8028(5)	27(2)
Br(1)	5000	7620(2)	6428(1)	36(1)

Table S3. Bond distances (Å) and angles [°] for **1**.

Sn(2)-O(2)	2.134(7)	Sn(1)-O(4)	2.146(6)
Sn(2)-O(1)	2.144(6)	Sn(1)-O(4)#1	2.146(6)
Sn(2)-O(1)#1	2.144(6)	Sn(1)-O(3)	2.143(7)
P(1)-O(1)#2	1.514(6)	P(2)-O(2)	1.475(8)
P(1)-O(1)	1.514(6)	P(2)-O(3)	1.497(8)
P(1)-H(1)	1.2799	P(2)-H(3)	1.2800
P(1)-H(2)	1.2801	P(3)-O(4)	1.497(6)
P(3)-O(4)#3	1.497(6)	P(3)-H(6)	1.2801
P(3)-H(5)	1.2800		
O(2)-Sn(2)-O(1)	86.2(2)	O(2)-P(2)-O(3)	120.1(5)
O(2)-Sn(2)-O(1)#1	86.2(2)	O(2)-P(2)-H(3)	83.2
O(1)-Sn(2)-O(1)#1	83.8(3)	O(3)-P(2)-H(3)	119.6
O(4)-Sn(1)-O(4)#1	83.4(3)	O(4)-P(3)-O(4)#3	117.8(5)
O(4)-Sn(1)-O(3)	86.9(2)	O(4)-P(3)-H(5)	106.5
O(4)#1-Sn(1)-O(3)	86.9(2)	O(4)#3-P(3)-H(5)	106.5
O(1)#2-P(1)-O(1)	114.9(5)	O(4)-P(3)-H(6)	95.6
O(1)#2-P(1)-H(1)	126.2	O(4)#3-P(3)-H(6)	95.6
O(1)-P(1)-H(1)	99.2	H(5)-P(3)-H(6)	135.8
O(1)#2-P(1)-H(2)	107.6	P(1)-O(1)-Sn(2)	134.1(4)

Symmetry transformations used to generate equivalent atoms: #1 -x+2,y,z; #2 -x+1,y,z; #3 -x+3,y,z.

Reference:

(1) Kresse, G.; Furthmuller, J. Efficient Iterative Schemes for ab initio Total-Energy Calculations using a Plane-Wave Basis Set. *Phys. Rev. B* **1996**, *54*, 11169-11186

(2) Perdew, J. P.; Burke, K.; Ernzerhof, M. Generalized Gradient Approximation Made Simple. *Phys. Rev. Lett.* **1996**, *77*, 3865-3868

(3) Blochl, P. E. Projector Augmented-Wave Method. *Phys. Rev. B* **1994**, *50*, 17953-17979

(4) Kresse, G.; Joubert, D. From Ultrasoft Pseudopotentials to the Projector Augmented-Wave Method. *Phys. Rev. B* **1999**, *59*, 1758-1775

(5) Sharma, S.; Ambrosch-Draxl, C. Linear and Second-order Optical Response from First Principles. arXiv:cond-mat/0305016v2

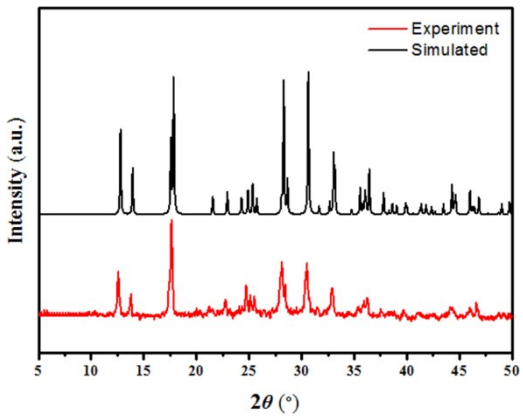

Fig. S1 Experimental and calculated powder X-ray diffraction patterns of **1**.

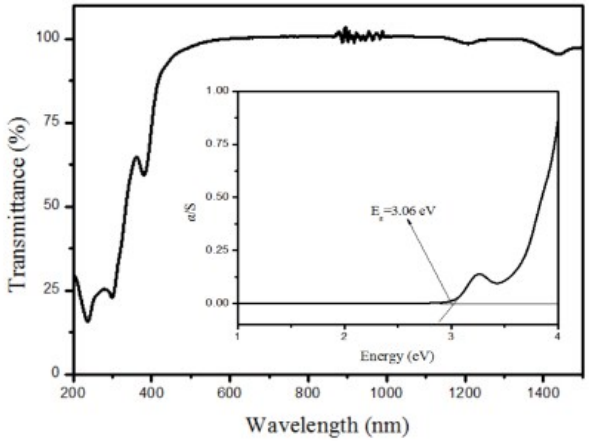

Fig. S2 UV-Vis-Near IR optical diffuse reflectance spectra for **1** .

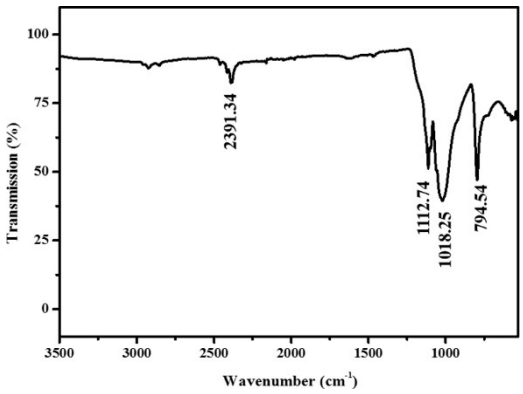

Fig. S3 FT-IR spectrum of **1**.

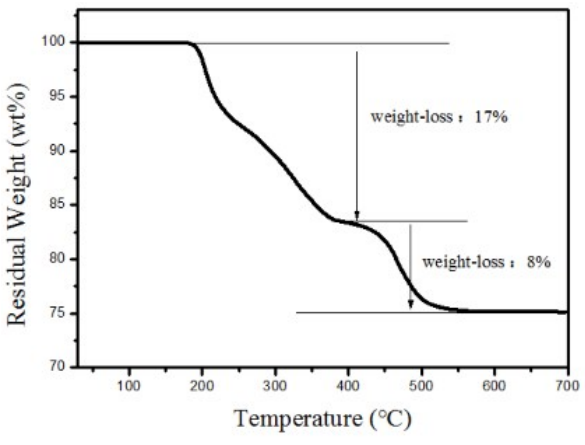

Fig. S4 TGA curve of **1**.

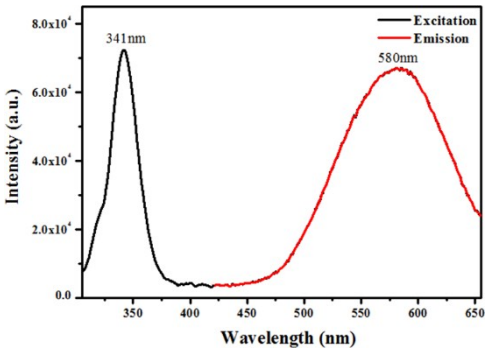

Fig. S5 Emission spectra of **1** in solid state at room temperature (λ_{ex} = 341 nm).

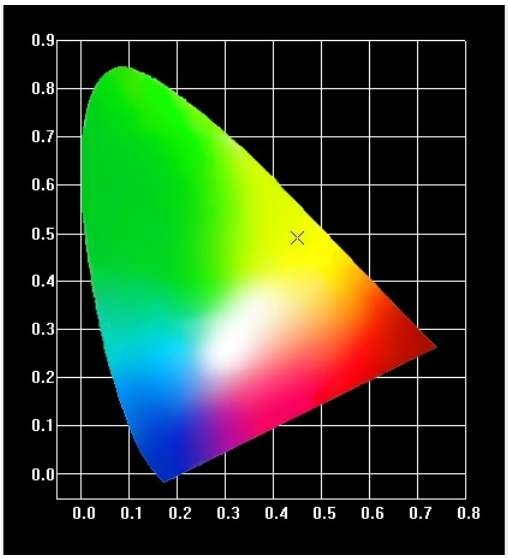

Fig. S6. The Commission Internationale de l'Eclairage (CIE) chromaticity coordinates of **1**.

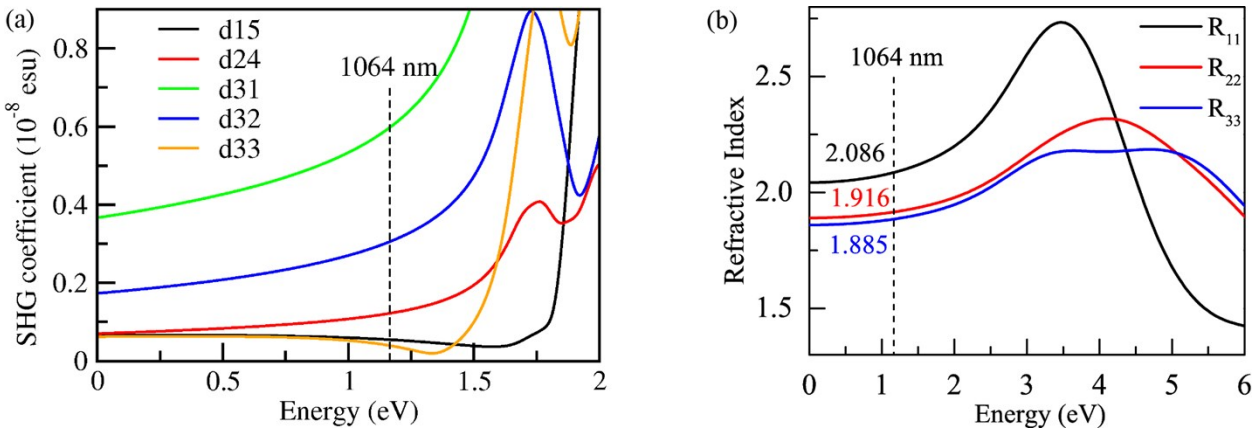

Fig. S7. (a) Frequency-dependent second harmonic generation susceptibility for compound **1**. (b) The calculated refractive index of the *xx*, *yy*, *zz* component (R_{11}, R_{22} and R_{33}) for compound **1**.